RAD Conference Proceedings, vol. 7, pp. 6-12, 2023
ISSN 2466-4626 (online) | DOI: 10.21175/RadProc.2023.02
www.rad-proceedings.org

NON-DESTRUCTIVE TESTING OF ALTERNATIVE MATERIALS FOR STORING RADIOACTIVE WASTE, USING COMPUTED 3D GAMMA TOMOGRAPHY

David Zoul*[1], Pavel Zháňal[1], Patricie Halodová[1], Antonín Kolros[1], Ladislav Viererbl[1], David Dobrev[2], Petr Večerník[2]

[1]Research Centre Rez, Czech Republic
[2]Nuclear Research Institute Rez, Czech Republic)

Abstract**.** *In May 2021, the SPE-CT facility for computed gamma tomography at the Research Centre Rez underwent its third major upgrade. One of the stated objectives was to assess the possibility of using the SPE-CT equipment for the TA CR TREND ALMARA project, which is the subject of this article. In this project, small cores of irradiated metals were cast into the studied fixation matrices. After matrix hardening, the possibility to determine by a non-destructive method the exact position of these coupons in the matrix was tested with the help of the device. The formation of corrosion products at the contact point between the two materials and the subsequent migration of radioisotopes in the matrix were also studied.*

Keywords: *gamma tomography, coeptor, sinogram, tomogram, Radon space, Fourier transform, pinhole camera, slit camera, convolution, Python code*

1. INTRODUCTION

One of the greatest advantages of computed tomography is the possibility of 3D imaging. This requires the application of a sufficient number of projections and the subsequent mathematical reconstruction of the image. The modification of the SPE-CT facility for computed gamma tomography at the Research Centre Rez in May 2021 enabled a previously unprecedented refinement of the method and, among other things, the extension of the static 3D display to include time-lapse recording, which provides information on, for example, the kinematics of groundwater migration processes in the geological subsoil of sites selected for the construction of a future permanent radioactive waste repository.

One of the objectives was to assess the possibility of using the SPE-CT equipment for the non-destructive determination of the exact position of the small cores of irradiated metals cast into the studied fixation matrices. The formation of corrosion products at the contact point between the two materials and the subsequent migration of radioisotopes in the matrix were also studied.

2. SPE-CT SCANNER

The 3D scanner was completed according to the technical design of the Research centre Rez in 2016. It includes a rotating sample clamp driven by a stepper motor (ϕ axis) and a two-row (x and y) scanning device with two stepper motors for scanning the transverse plane of the sample (x-axis) and for moving the detector in the longitudinal direction of the sample (y-axis), as shown in Figure 1.

The instrument, with a resolution of greater-than-one cubic millimetre, provides a 3D view into the interior of small radioactive samples with diameters on the order of units to tens of millimetres. The device is designed to show the spatial distribution of radioactivity within samples. It uses radiation emitted by the sample itself, which is first closely collimated and then detected.

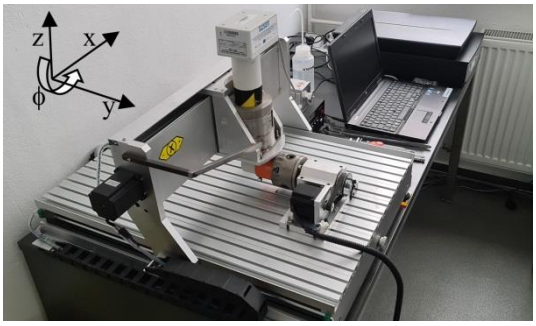

Figure 1. SPE-CT scanner

2.1. Detection and collimation system (SPE-CT camera)

The detection system (Figure 2) consists of a microprocessor-controlled REP171-ISD intelligent scintillation probe, with a regulated HV source and current and frequency converter, equipped with an encapsulated $CdWO_4$ scintillation detector: ø 10 mm and length 30 mm, selected for its ^{60}Co gamma

* E-mail of the corresponding author – david.zoul@cvrez.cz

detection efficiency. (Its length was optimized for complete gamma absorption, and the small diameter was optimal for signal-to-background ratio). Furthermore, the photomultiplier operates in current mode, i.e. without dead time. The dynamic response measurement is five orders of magnitude without switching, and measurement uncertainty is approximately 2%.

Figure 2. Scintillation detector with collimation system components

The collimation system (Figures 2 and 3) consists of a modular tungsten collimator: ø 97 mm and height 45 mm + 55 mm, with an optional circular aperture: ø 1 mm or 2 mm, or slit 20 x 1 mm, flexibly optimizing the ratio between resolution and signal-to-noise-ratio (SNR) depending on the physical characteristics of the sample.

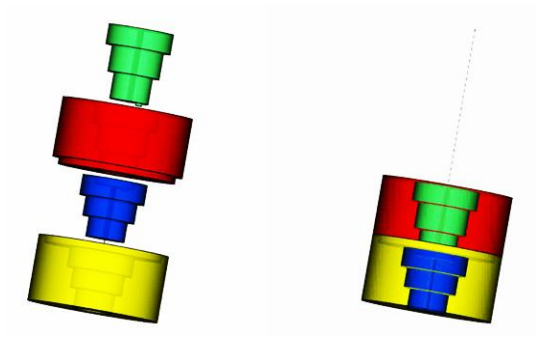

Figure 3. Modular tungsten collimator

2.2. Coeptor

In May 2021, the gamma tomograph was upgraded, motivated by the idea of moving from conventional 3D scanning to 4D scanning, which requires an order of magnitude higher for the number of projections. The aim was to develop and install a device (called a coeptor, from the Latin coeptus: beginning) that radiatively marks the beginning of each line in the sinogram with a distinct peak in the output vector generated by the scintillation detector.

The coeptor consists of a small, sealed source of ^{241}Am with an activity of 5 MBq. The alpha radiation of this radionuclide, with a half-life of 432 years, is already completely absorbed by the silver exit window of the coeptor. Only the gamma radiation with an energy of 59.5 keV penetrates outside the coeptor and is absorbed by the 40 mm-thick tungsten shielding of the scintillation detector. However, a small hole with a 4 mm diameter has been drilled in the shielding, through which this radiation penetrates unhindered by the detector if the coeptor is located directly in front of the hole, per Fig. 4.

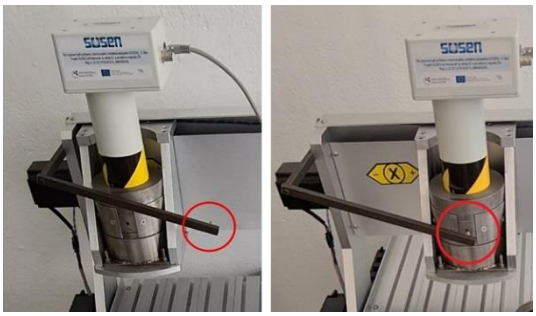

Figure 4. Coeptor

Before starting to scan each new line, the detector briefly passes through this aperture in front of the coeptor output window, creating a distinct peak in the record with a height of over 100 CPS and a FWHM of several seconds, per Figure 5.

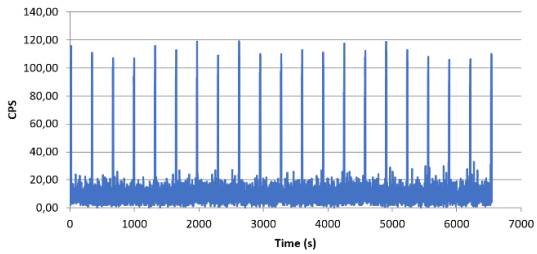

Figure 5. Record of the detector's response during its periodic crossing over the exit window of the coeptor

3. Corrosion and interaction experiments

One of the set objectives was to assess the possibility of using SPE-CT equipment to study the formation of corrosion products of small coupons of activated metals embedded in a fixation matrix (at the contact point of these materials), and the migration of individual radioisotopes in the matrix.

Irradiated steel of approximately 1 mm × 3 mm × 10 mm and titanium grit of 0.63–1 mm fraction were used for corrosion and interaction experiments (Figure 6). The irradiation of the samples was conducted using the research reactor LVR-15 of the Research Centre Rez.

Cement and geopolymer matrices were chosen for fixation of real samples of active materials. The

metallic materials were registered, weighed and placed in polystyrene tubes. Approximately 2 ml of the fixation matrix, cement or geopolymer paste was then

Figure 6. Left – irradiated steel coupon; Right – irradiated titanium scrap

added to the tubes. After homogenization, the matrices hardened to form small capsules with incorporated metallic materials of approximately 10 mm diameter and 20 mm height, as shown in Figure 7, Left.

The capsules were then fixed into a final experimental body made of cement or geopolymer matrix in the shape of a cylinder with a diameter of 50 mm and a length of 50 mm.

The aim was to place the capsule in the centre of the experimental solid. For the selected cement and geopolymer matrix bodies, the placement was verified at the Institute of Archaeology, Prague, Czech Republic, using radiography (Figure 7, Middle).

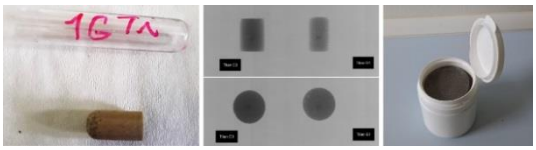

Figure 7. Left – a capsule made of fixation geopolymer matrix 10 mm in diameter and 20 mm long, with incorporated titanium grit; Middle – X-ray photograph of experimental bodies with titanium grit fixed in cement and geopolymer matrix, the side view and top view determining the position of the capsule with incorporated Ti grit; Right – a plastic capsule with an experimental body immersed in a solution of synthetic granitic water (type SGW 3) pH 12, under anaerobic conditions and in a glove box with an argon atmosphere

Subsequently, the experimental bodies were immersed in a solution of synthetic granitic water (type SGW 3) of pH 12, under anaerobic conditions in an argon glove box, and left there exposed for one year (Figure 7, Right). After their removal from the solution, the bodies were dried, cleaned, labelled and subjected to gamma-spectrometric, dosimetric and gamma-tomographic analyses on an SPE-CT scanner.

4. Gamma-spectrometric characterization of samples

Gamma-spectrometric characterization of both types of metal cores was conducted by a gamma-spectrometric line with the high purity germanium (HPGe) detector GEM10-70-PL, from ORTEC. Table 1 summarizes the results of the gamma spectrometry.

5. Non-destructive SPE-CT analyses

In 2022, 3D scanning with the SPE-CT was used for the first time to accurately determine the position of irradiated metal cores within a geopolymer matrix. In the future, there is also the possibility of 4D scanning

Table 1. Gamma-spectrometric characteristic 1

Sample	Surface dose equivalent rate (μSv/h)	Total emission (s^{-1})	Estimated activity (kBq)
4G	1.5	11,541	21
4C	1.5	15,072	21
6	110	965,204	1,356
8	110	1,114,245	1,570

at intervals of several months to years to determine whether radioactivity is migrating from the metal cores into the matrix over time, or even to determine the rate of such migration.

The first series of analyses were conducted with inactive samples in the second half of 2022. The scanning of radioactive samples in this project was conducted in mid-December 2022.

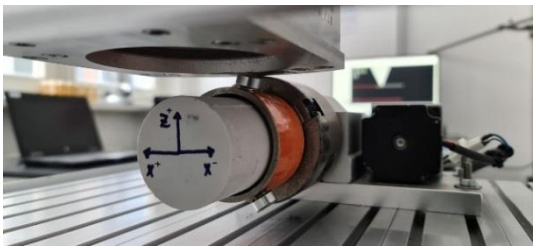

Figure 8. Geopolymer test body fixed in the SPE-CT scanner rotary fixture

5.1. The principle of single-photon emission computed tomography (SPE-CT)

The ability to scan and subsequently reconstruct a 3D map of the activity distribution within the sample provides highly useful information about its internal structure. This requires the application of a sufficient number of projections and subsequent mathematical reconstruction of the image.

The scanning of the sample occurs in the transverse plane of the sample (x-axis). The first set of values for one scan is obtained. Then, the whole sample is rotated by a fixed angle ϕ, and the scan is repeated. The sample is then rotated 360°, and the slice image is computationally reconstructed.

Each scan (the set of values obtained for one particular rotation angle of the sample) forms one line of the so-called sinogram – the Fourier image of the scanned slice, in the so-called Radon space. The individual rows (for different sample angles) then form a matrix of values representing the entire sinogram.

To create a 3D image of the entire sample, after each complete sinogram is acquired, the detector is always shifted by a discrete step in the longitudinal direction of the sample (y-axis), and the scanning sequences are repeated. A sequential group of

sinograms, one for each section of the sample, is thus obtained [1] – [5].

By applying a low-pass convolution filter, the noise is first filtered out of the sinograms, and then the original 3D image of the scanned object is reconstructed by backward Fourier transformation [6] – [8].

5.2. Non-destructive analysis using a pinhole camera

The scanning algorithm took 26 hours using a collimator with a circular aperture of 2 mm diameter (the so-called pinhole camera) and a scanning head feed rate of 20 mm per minute. The Fourier images of the two tested samples – Sample 8 (irradiated steel in cement matrix) and Sample 6 (irradiated steel in geopolymer matrix) – are shown in Figure 9. The sinogram lines correspond to the displacement of the SPE-CT camera in the horizontal x-axis perpendicular to the sample axis. Their length corresponds to a cement cylinder diameter of 50 mm; thus, a density of 166 pixels per line provides a resolution of approximately 0.3 mm in directions perpendicular to the sample axis. Scanning started at a rotation angle ϕ of the sample coordinate system (marked on the sample with an alcohol marker) of 18°, and ended at a rotation angle of 360° = 0°, with a step of 18°. Thus, each sinogram has a total of 20 lines corresponding to each rotation angle.

The first sinogram corresponds to a cut through the smooth face of the cylinder, which represents the bottom of the mould into which the matrix was poured. The last sinogram corresponds to a cut approximately 10 mm below the surface of the casting (the rough face of the cylinder at the opposite end). The cylinder was held in a rotating fixture by this section, so it was scanned no further. One step in the y-axis corresponded in real terms to 2 mm; a total of 20 sinograms were obtained, i.e. an area of 40 mm was scanned along the axis of the cylinder, from its face to the clamping device. Figure 9 presents all 20 sinograms, some of which clearly show the signal from the metal cores inside.

Due to the relatively high surface dose equivalent rate, the Fourier image of the steel core inside is well defined, and its position can be determined to within 1 mm. However, it appears to be lined by an active layer of up to 5 mm wide in places, which could indicate that radioactivity has already started to spread from the nuclei to the surroundings. Although the fringe may also be a mere artefact of convolution, it is much wider (the 3 x 3 convolution kernel blurring the pixels to roughly twice or three times their original size, which still gives a resolution greater than 1 mm), and traces of radioactivity are also clearly visible in the two adjacent sections at either end of the sample, which (given the 2 mm step length in the y-axis direction) are no longer demonstrably free of the sample.

It is clear that, compared to Sample 8, which is practically in the axis of the cylinder with its lower end (closer to the smooth face of the cylinder) and is offset by about 3 mm from the axis of the cylinder with its upper end, the alignment of the entire Sample 6 is at least 6 mm. While in Sample 8 the core lies at a depth of 16 mm to 26 mm from the smooth face of the cylinder, in Sample 6 it is 12 mm to 22 mm. In other respects, the two samples are highly similar.

The reconstruction of the slices from the sinograms was realized by the backward Fourier transform in the computational Python code. This transformation converts the recording from Radon space back to object space. The result is therefore 20 slices (so-called tomograms) of the sample, corresponding to the original 20 sinograms. To increase the quality of the display, the individual reconstructed slices were further convolved with a Gaussian filter. The results for the individual studied samples can be viewed in Figure 10.

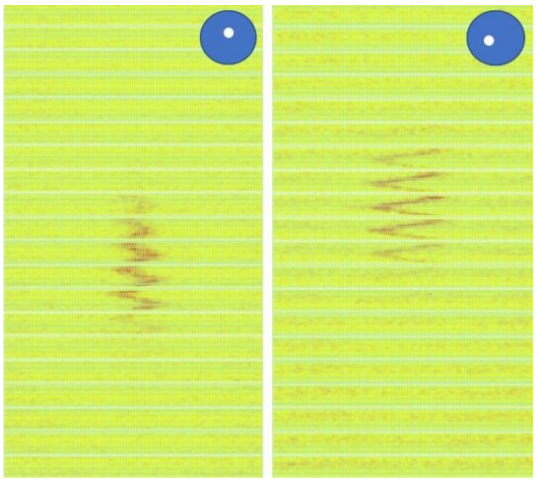

Figure 9. Filtered sinograms of Sample 8 (Left) and Sample 6 (Right), showing the signal from the inner steel cores. In the upper right corner, the estimated position of the metal core in the sample is marked with a white dot.

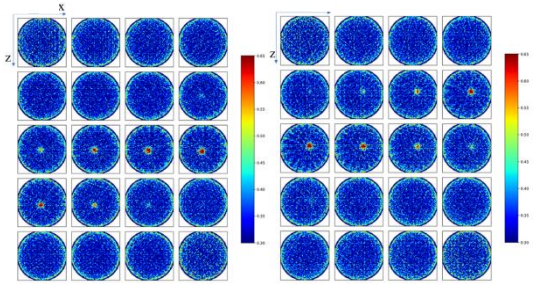

Figure 10. Inverse Fourier transform sinograms of Sample 8 (Figures. 9 and 10, Left) and Sample 6 (Figures. 9 and 10, Right) showing individual sections (tomograms) of the sample with a clear image of the radioactive steel core inside (shades of red). A resolution of each tomogram: 180 pixels x 180 pixels, diameter: 50 mm.

5.3. Non-destructive analysis using a slit camera

The surface dose equivalent rates of titanium Samples 4G (titanium in geopolymer matrix) and 4C (titanium in cement matrix), at the time of measurement, were two orders of magnitude lower than the surface dose equivalent rates of the steel cores, so that the SNR of the pinhole camera scan was much smaller than the fluctuation of the radiation background. Therefore, only random noise was evident in the recording.

As such, a slit tungsten collimator with a slit width of 2 mm and a length of 20 mm was used for scanning in the next step. First, a hyperfine scan (feed rate of 1 mm per minute) was performed in the xϕ plane with the slit plane perpendicular to the x-axis, as shown in Figure 11, Left. Baseline sinograms were obtained (see Figure 12), showing a clear image of a greater, 10 mm wide titanium core displaced in both cases, about 10 mm off the cylinder axis.

This was followed by a hyperfine scan in the yϕ plane with the slit rotated 90° (perpendicular to the sample axis this time), which provided weighting factors for each row (ϕ) of each sinogram, depending on its position (y), per Figure 11, Right.

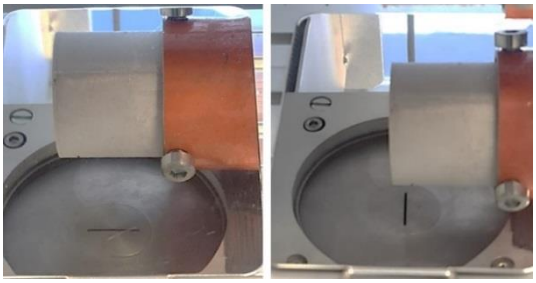

Figure 11. Specular reflection of a slit SPE-CT camera, with a slit oriented parallel (Left) and perpendicular (Right) to the rotation axis of the sample

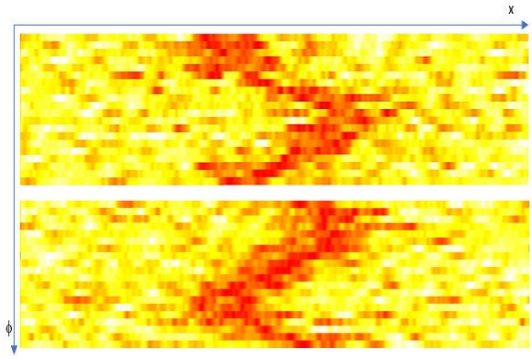

Figure 12. Basic sinograms of titanium cores inside the geopolymer (Top) and cement (Bottom) matrix, taken with a slit SPE-CT camera with a 20 mm x 2 mm slit oriented perpendicular to the x-axis, moving in the plane xϕ

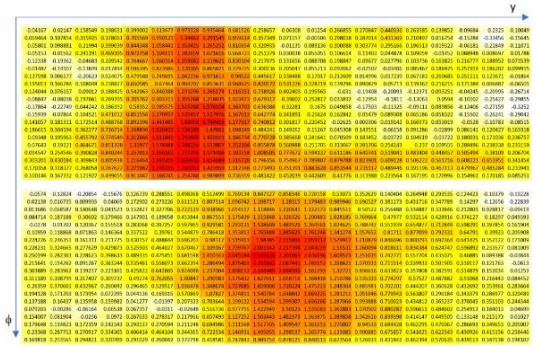

Figure 13. Weight matrix of 20 x 20 titanium core in geopolymer matrix (Top) and of a titanium core in a cement matrix (Bottom), 'smoothed' by a low-pass filter represented by a 3 x 3 convolution kernel. The columns comprise weight vectors corresponding to each specific position of the SPE-CT camera slit on the y-axis, and the rows correspond to different angles ϕ of sample rotation.

These weighting factors were obtained as the differences between the detector signal (pulse rates) corresponding to each specific position yϕ and the average value of the radiation background, as shown in Figure 13.

The weighting factors were successively multiplied by the corresponding rows of the sinograms from Figure 12. Each row separately had to be further normalized with respect to the other sinograms by adding a constant K such that the P value of the average radiation background multiplied by the corresponding weight V gave P again after adding K, or as follows:

$$P \cdot V + K = P \qquad (1)$$

Hence,

$$K = P(1 - V) \qquad (2)$$

Thus, all 20 sinograms forming the Fourier image of the whole 3D sample were reconstructed in turn, per Figure 14. Apart from the already mentioned alignment of the titanium core in the geopolymer by approximately 10 mm, the image clearly shows its position on the y-axis, which, measured from the smooth face of the cylinder, is only 8 mm to 18 mm. The position on the y-axis of the titanium core in the cement is 16 mm to 26 mm from the smooth face of the cylinder, and its offset is also 10 mm. There are also faint recurring artefacts ('ghosts' or 'echoes') in the images, which are due to the computational method

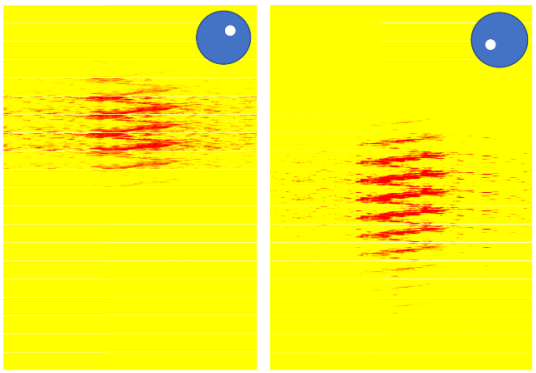

Figure 14. Record of 20 sinograms of the titanium core in the geopolymeric matrix (Left) and of a titanium core in a cement matrix (Right), taken with a 20 mm x 2 mm slit SPE-CT camera. In the upper right corner, the estimated position of the metal core in the sample is marked with a white dot.

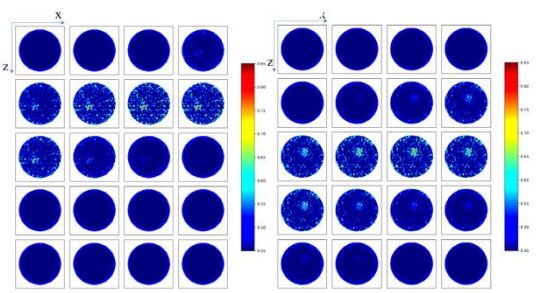

Figure 15. Inverse Fourier transform sinograms of Sample 4G (Figures. 14 and 15, Left) and Sample 4C (Figures. 14 and 15, Right) showing individual sections (tomograms) of the sample with a clear image of the radioactive titanium core inside (shades of red). A resolution of each tomogram: 180 pixels x 180 pixels, diameter: 50 mm.

used. Their maximum elimination will be the subject of further refinement of the method.

The developed method of reconstructing the Fourier image from the data obtained with the slit SPE-CT camera has enabled at least an order of magnitude increase in the sensitivity of gamma tomographic detection. Due to the insignificant emission of radiation from the sample surface (approximately 10,000 s^{-1}), the result, presented below, can be considered a major breakthrough of the limit of applicability of the whole SPE-CT method.

5.4. Reconstruction of 3D objects

By combining all 20 tomograms in space, the resulting 3D reconstruction of the scanned objects was obtained, per Figure 16.

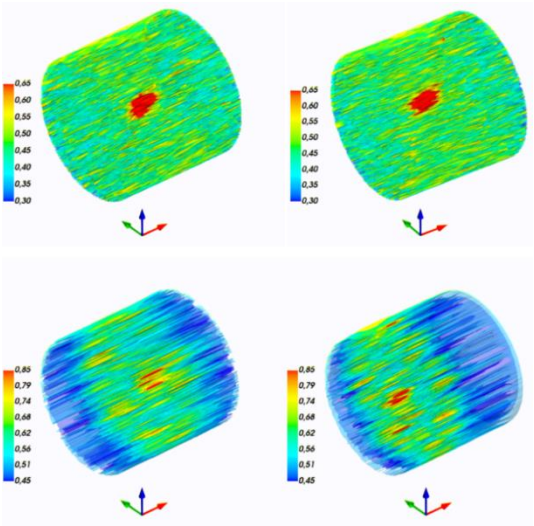

Figure 16. Tomographic 3D reconstruction of sample no. 8 (Top Left), no. 6 (Top Right), no. 4G (Bottom Left) and no. 4C (Bottom Right) at x, y, z scale, equalling 10 mm

In Figure 17, the detected region of migrating radioactivity diffusing from the steel core into the matrix is shown with dashed lines.

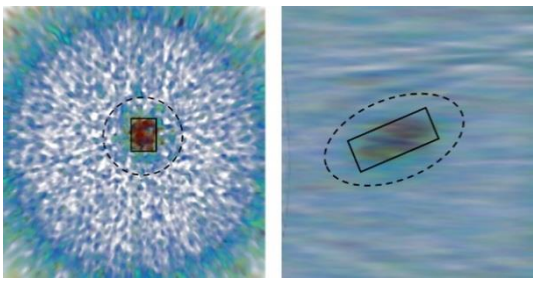

Figure 17. Close-up of radioactivity migrating into the cement matrix (dashed line) around the steel core (solid line)

6. Conclusion

Gamma tomography of radioactive samples from the TA CR TREND ALMARA project has demonstrated the usefulness of the SPE-CT device for non-destructive analysis of the position and shape of small metallic coupons of radioactive metals embedded in a fixation matrix, possibly also for the study of the release of corrosion products from these coupons at the contact point between the two materials, and the migration of radioisotopes in the matrix.

For all the samples analysed, the position and dimensions of the metal nuclei in the matrix could be determined accurately. Furthermore, indications were found that some radioactivity had migrated from the steel cores into the matrix, up to a distance of 5 mm. Verification of this fact will be the subject of further destructive analyses and will be highly important for the future development of this tomographic method.

No migration of radioactivity into the matrix has been demonstrated for the titanium cores, which may be a consequence of the already low activity of these cores at the time of the gamma tomographic scan. Nevertheless, a significant milestone in the sensitivity of gamma tomography scanning was achieved in this case, as it was possible to reconstruct accurately the position of metal nuclei in the matrix using a slit-type SPE-CT camera, offering an SNR an order of magnitude higher than that of a conventional pinhole camera.

In contrast to the smooth and compact cupules seen inside Samples 6 and 8, the reconstructed images of Sample 4 clearly show that the cores have a granular consistency and are a heterogeneous crumb.

The developed method of image reconstruction from gamma tomography with a slit SPE-CT camera opens up completely new possibilities for non-destructive testing, such as 4D scanning of low-activity (on the order of kBq) rock, building material or other porous samples directly inside diffusion cells, with the aim of time-lapse recording of radioactive tracer penetration through the sample.

Acknowledgements: *The presented results were implemented with the state support of TA CR as part of the TREND ALMARA programme, project number FW01010115. Alternative materials for storing radioactive waste were NPP decommissioning.*

References

1. J. Radon, "On the determination of functions from their integral values along certain manifolds", *IEEE Transactions on Medical Imaging*, **5**(4), 170-176, 1986. https://doi.org/10.1109/TMI.1986.4307775
2. A. Cormack, "Representation of a function by its line integrals with some radiological implications I", *J. Appl. Phys.*, **34**(9), 2722–2727, 1963. https://doi.org/10.1063/1.1729798
3. A. Cormack, "Representation of a function by its line integrals with some radiological implications II", *J. Appl. Phys.*, **35**, 2908–2918, 1964. https://doi.org/10.1063/1.1713127
4. G. F. Knoll, "Single-photon emission computed tomography", *Proc. IEEE*, **71**(3), 320–329, 1983.

https://doi.org/10.1109/PROC.1983.12590

5. A. C. Kak, M. Slaney, "Principles of Computerized Tomographic Imaging", *IEEE Press*, 1988. https://doi.org/10.1137/1.9780898719277
6. M. Dogan et al. "Tomography imaging of technetium transport within a heterogeneous porous media", *Environ. Sci. Technol.*, **51**(5), 2864–2870, 2017. https://doi.org/10.1021/acs.est.6b04172
7. D. Zoul, P. Zháňal, "3D reconstruction of radioactive sample utilizing gamma tomography", *Nucl. Instr. Meth. Phys. Res. A*, **859**, 107–111, 2018. https://doi.org/10.1016/j.nima.2018.03.071
8. D. Zoul, P. Zháňal, L. Viererbl, A. Kolros, M. Zuna, V. Havlová, "3D reconstruction of inner structure of radioactive samples utilizing gamma tomography", *Radiation Protection Dosimetry*, **186**(2-3), 239-243, 2019. https://doi.org/10.1093/rpd/ncz211